arXiv:0804.0350v1 [hep-ph] 2 Apr 2008

NLO QCD corrections to tri-boson production

T. Binoth[a]**, G. Ossola**[b]**, C. G. Papadopoulos**[b]**, and R. Pittau**[c]

[a] *The University of Edinburgh, School of Physics, Edinburgh EH9 3JZ, UK*

[b] *Institute of Nuclear Physics, NCSR Demokritos, 15310 Athens, Greece*

[c] *Departamento de Física Teórica y del Cosmos, CAPFE, Universidad de Granada, E-18071 Granada, Spain*

ABSTRACT: We present a calculation of the NLO QCD corrections for the production of three vector bosons at the LHC, namely ZZZ, W^+W^-Z, W^+ZZ, and $W^+W^-W^+$ production. The virtual corrections are computed using the recently proposed method of reduction at the integrand level (OPP reduction). Concerning the contributions coming from real emission we used the dipole subtraction to treat the soft and collinear divergences. We find that the QCD corrections for these electroweak processes are in the range between 70 and 100 percent. As such they have to be considered in experimental studies of triple vector boson production at the LHC.

KEYWORDS: NLO Computations, QCD, Hadronic Colliders, Standard Model.

Contents

1. Introduction

For TeV collider physics hard multi-particle final states are ubiquitous and theoretical calculations can not provide reliable predictions without taking into account higher order information. Unfortunately the evaluation of one-loop amplitudes with many external particles is technically very challenging, which motivated a priority list for one-loop computations relevant for the Large Hadron Collider at CERN, the so called Les Houches wish list [1]. Due to the relevance for LHC phenomenology many new avenues have been explored in the last few years, ranging from evaluation techniques of Feynman diagram [2, 3, 4, 5, 6] to unitarity based approaches [7] in different variations [8, 9, 10, 11, 12, 13, 14, 15].

Higher order QCD results have been provided recently for multi-boson production $pp \rightarrow ZZZ, WWZ, HHH$ processes [16, 17, 18, 19], in the context of weak boson fusion [20, 21, 22, 23, 24], $pp \rightarrow Hjj$ with effective gluon-Higgs couplings [25], $gg \rightarrow Hq\bar{q}$ [26], and $pp \rightarrow t\bar{t}j$ [27].

In two recent papers [28, 29], a new technique (OPP) has been introduced for the reduction of arbitrary one-loop sub-amplitudes at *the integrand level* [30] by exploiting numerically the set of kinematical equations for the integration momentum, that extend the quadruple, triple and double cuts used in the unitarity-cut method [31, 32, 33]. The method requires a minimal information about the form of the one-loop (sub-)amplitude and therefore it is well suited for a numerical implementation.

In the present work, the OPP reduction is applied to the calculation of the next-to-leading order QCD correction for the production of three vector bosons at the LHC. This includes the case of ZZZ production, as well as the W^+W^-Z, W^+ZZ, and $W^+W^-W^+$ production. The physics motivation for a reliable prediction of these processes is two-fold: firstly one is sensitive to quartic vector boson couplings and secondly the leptonic decays are prominent Standard Model backgrounds for multi-lepton and missing energy signatures present in many new physics scenarios.

As the triple vector boson production is genuinely an electroweak process one can not expect that the inclusion of QCD effects leads to the reduced scale dependence typically seen in this kind of calculations. In contrary it can be qualitatively understood that the LO predictions show a relatively small sensitivity when varying the factorisation scale. This is because the parton distribution functions are called for x-values which are around the scaling region where one has a very mild Q^2-dependence. After adding the order α_s corrections one expects to observe a LO type scale variation in the added contribution.

The production of three Z bosons has already been discussed by Lazopoulos et al. in Ref. [16]. We also presented some preliminary results in Refs.[1, 34]. The W^+W^-Z case has been studied in Ref. [17] for all combinations of leptonic final states. Results for W^+ZZ and $W^+W^-W^+$ production have not been presented in the literature yet.

Our calculation is composed of two main parts: the evaluation of virtual corrections, namely one-loop contributions obtained adding a virtual particle to the tree-level diagrams, and corrections from the real emission of one additional massless particles from initial and final states, needed in order to control and cancel infrared singularities. The virtual corrections are computed using the `OPP` reduction [28, 29]. In particular, we make use of `CutTools` [35], a FORTRAN90 code that implements the general method of reduction. Concerning the contributions coming from real emission we used the dipole subtraction method [36] to isolate the soft and collinear divergences and checked the results using the phase space slicing method [37, 38] with soft and collinear cutoffs, as outlined in [39, 40].

The paper is organized as follows. In Section 2, we report the details of the calculation of the virtual part. Section 3 is devoted to the discussion of soft and collinear singularities. In Section 4, we show our results, including transverse momentum and rapidity distributions for the different

processes studied in this paper. Finally, in Section 5, we will give a summary of the work done and present our conclusions.

2. Virtual corrections

We consider the process

$$q(p_1) + \bar{q}(p_2) \longrightarrow V(p_3) + V(p_4) + V(p_5) \tag{2.1}$$

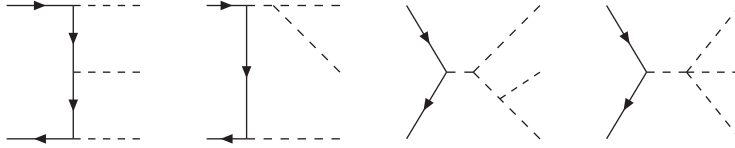where $V = Z, W$. All momenta are chosen to be incoming, such that $\sum_i p_i = 0$.

Figure 1: Tree-level structures of Feynman diagrams contributing to $q\bar{q} \to VVV$, where $V = Z, W$. Dashed internal lines can represent W, Z, Goldstone bosons or photons.

At the tree-level, diagrams can be grouped in four different topologies, which are illustrated in Fig. 1. One-loop corrections are obtained by adding a virtual gluon to the tree-level structures, as depicted in Figs. 2 and 3.

We perform a reduction to scalar integrals using the OPP reduction method [28, 29]. In this approach, we need to provide the numerical value of the numerator of the integrand in the loop integrals. We refer to it as the numerator function $N(q)$, where q is the integration momentum.

The numerator function $N(q)$ can be expressed in terms of 4-dimensional denominators $D_i = (q + p_i)^2 - m_i^2$ as follows

$$
\begin{aligned}
N(q) = &\sum_{i_0 < i_1 < i_2 < i_3}^{m-1} \left[d(i_0 i_1 i_2 i_3) + \tilde{d}(q; i_0 i_1 i_2 i_3) \right] \prod_{i \neq i_0, i_1, i_2, i_3}^{m-1} D_i \\
&+ \sum_{i_0 < i_1 < i_2}^{m-1} \left[c(i_0 i_1 i_2) + \tilde{c}(q; i_0 i_1 i_2) \right] \prod_{i \neq i_0, i_1, i_2}^{m-1} D_i \\
&+ \sum_{i_0 < i_1}^{m-1} \left[b(i_0 i_1) + \tilde{b}(q; i_0 i_1) \right] \prod_{i \neq i_0, i_1}^{m-1} D_i \\
&+ \sum_{i_0}^{m-1} \left[a(i_0) + \tilde{a}(q; i_0) \right] \prod_{i \neq i_0}^{m-1} D_i .
\end{aligned} \tag{2.2}
$$

The quantities $d(i_0i_1i_2i_3)$ are the coefficients of 4-point scalar functions with denominators labeled by i_0, i_1, i_2, and i_3. In the same way, $c(i_0i_1i_2)$, $b(i_0i_1)$, and $a(i_0)$ are the coefficients of the 3-point, 2-point and 1-point scalar functions, respectively. The other quantities appearing in Eq. (2.2), marked with a "tilde", vanish upon integration over q. Such a separation is always possible and the set of coefficients d, c, b, a is immediately interpretable as the ensemble of the coefficients of all possible 4, 3, 2, 1-point one-loop functions contributing to the amplitude.

Since the structure of Eq. (2.2) is general, namely independent from the particular process that we want to study, the task of computing the one-loop amplitude is then reduced to the algebraical problem of fitting the coefficients d, c, b, a by evaluating the function $N(q)$ a sufficient number of times, at different values of q, and then inverting the system. That can be achieved quite efficiently by singling out particular choices of q such that, systematically, 4, 3, 2 or 1 among all possible denominators D_i vanishes. Then the system of equations is solved iteratively [1].

First one determines all possible 4-point functions, then the 3-point functions and so on. In summary, simply by evaluating the numerator function $N(q)$ for a given set of values of q, we can extract all the coefficients in Eq. (2.2).

As a possible future development, the numerical evaluation of $N(q)$ could be performed automatically without relying on Feynman diagrams, by means of recursion relations. For the current project however, we still follow the traditional approach of computing all the expression originating from Feynman diagrams, and use them to evaluate numerically the numerator functions. An example in Section 2.1 will clarify the details of the technique used.

The coefficients determined in this manner should be multiplied by the corresponding scalar integrals. Since, in the process that we are studying, no q-dependent massive propagators appear, we will only need massless scalar integrals. They are computed using the package `OneLOop` written by A. van Hameren [5].

The last step is the calculation of the rational terms. As explained in Ref. [42], there are two sources of the rational terms: a first contribution, that we call R_1, originates from considering the fact that the denominators appearing in the scalar integrals are n-dimensional objects, while the expansion of Eq. (2.2) is purely 4-dimensional. These contributions can be automatically extracted in the reduction process, either by computing extra-integrals as explained in Ref. [29], or by means of a modified version of Eq. (2.2) in which the numerator function is expressed directly in terms of n-dimensional denominators. The second approach is illustrated in Ref. [42] and implemented in the package `CutTools` [35]. We checked that the results obtained for R_1 with the two methods are in perfect agreement.

The second contribution, that we call R_2, is instead originating from the numerator function.

---

[1]A method to optimize the solution of the system has been very recently presented in [41].

For many processes, $N(q)$ can be treated as a purely four-dimensional object. However, in general, it should be written as $\bar{N}(q) = N(q) + \tilde{N}(q^2, \epsilon)$, where $\bar{N}(q)$ is the n-dimensional numerator function. $\tilde{N}(q^2, \epsilon)$ can originate, for example, from the contraction of Dirac matrices or from powers of q^2 in the numerator function [43] and vanishes in the $\epsilon \to 0$ limit. In Ref. [42] we discussed in detail this topic and showed how R_2 can be obtained, for example, by using a set of tree-level like Feynman rules. For the calculation presented in this paper, however, it is easy to extract these remaining rational parts directly.

2.1 ZZZ production

In this subsection we describe the evaluation of the virtual QCD corrections to the process $q\bar{q} \to ZZZ$. The virtual part of the calculation involves eight different diagrams, which have been depicted in Fig. 2. Each diagram should be evaluated for six permutations of the final particles.
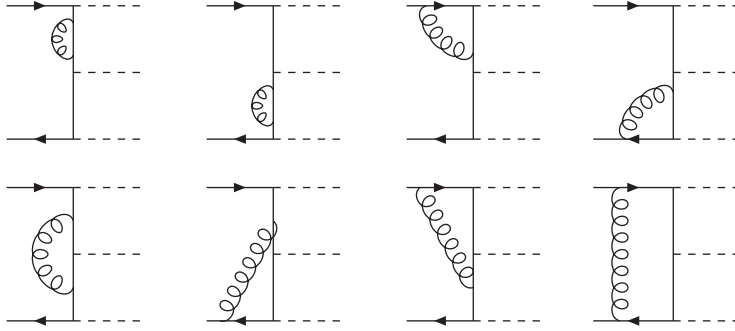

Figure 2: Diagrams contributing to virtual QCD corrections to $q\bar{q} \to ZZZ$

As an example, let us consider the pentagon diagram (the last diagram of Fig. 2). In our notation, the integrand will read

$$A_5(q) = \frac{N_5(q)}{[q^2][(q + p_1)^2][(q + p_1 + p_5)^2][(q - p_2 - p_3)^2][(q - p_2)^2]} \tag{2.3}$$

with

$$N_5(q) = \left\{ \bar{u}(p_2)\, \gamma^\alpha\, P_{(q-p_2)}\, V_3^Z\, P_{(q-p_2-p_3)}\, V_4^Z\, P_{(q+p_1+p_5)}\, V_5^Z\, P_{(q+p_1)}\, \gamma^\alpha\, u(p_1) \right\} \tag{2.4}$$

The function $P(q)$ is the numerator of the quark propagator

$$P_{(q)} = \slashed{q}\,,$$

while $V_i^Z = V^Z \cdot \epsilon_i$, namely the contraction between the polarization vector of the i-th Z boson ϵ_i and the γ-matrix in the vertex $Zq\bar{q}$

$$V_\mu^Z = ie\gamma_\mu(g_f^- \omega_- + g_f^+ \omega_+) \tag{2.5}$$

where

$$g_f^+ = -\frac{s}{c}Q_f \ , \ \ g_f^- = \frac{I_{W,f}^3 - s^2 Q_f}{sc} \ , \ \ \omega_\pm = (1 \pm \gamma^5)/2 \,, \ s = \sin\theta_W \,, \ c = \cos\theta_W. \qquad (2.6)$$

For any fixed value q_0 of integration momentum, and for a given phase space point, $N_5(q_0)$ is simply the trace of a string of known matrices. After choosing a representation for Dirac matrices and spinors, we evaluate $N(q)$ by performing a naive matrix multiplication. By providing this input to the reduction algorithm, we can compute all the coefficients of the scalar integrals (in other words, the "cut-constructible" part of the calculation).

In the same fashion, we can repeat the calculation for the other seven diagrams. However, our method allows for a further simplification: for each fixed permutation of the final legs, only the q-dependent denominators of Eq. (2.3) will appear also in the remaining diagrams. Therefore, we can combine all diagrams in a single numerator function and perform the reduction directly for the sum of such diagrams, allowing for a one-shot evaluation of the resulting scalar coefficients.

We checked that our results, both for poles and finite parts, agree with the results obtained by the authors of Ref. [16].

2.2 W^+W^-Z production

With the same technique we also evaluated the virtual QCD corrections to the process $q\bar{q} \to W^+W^-Z$. The structure of the diagrams is more involved with respect to the ZZZ case. There are in fact 19 different tree level diagrams. Adding QCD corrections, we obtain 58 one-loop diagrams contributing to this process. In addition to the structures already depicted in Fig. 2, in this case we can also have the diagrams appearing in Fig. 3.

A very similar calculation has been presented recently by Hankele and Zeppenfeld [17]. They studied the NLO QCD corrections to the production of 6 leptons in hadronic collisions, via WWZ production. A comparison with their results, however, is not straightforward and has not been performed yet.

2.3 W^+ZZ production

Concerning the production of W^+ZZ, we have 15 tree-level diagrams, which, after adding QCD corrections, give rise to 69 diagrams at NLO. Since in this process we generate a single charged W^+, the initial state should be of the type $u\bar{d}$ (rather then $u\bar{u}$ as for W^+W^-Z and ZZZ).

2.4 $W^+W^-W^+$ production

Starting again from an initial state of the type $u\bar{d}$, we should consider 15 diagrams at the tree-level and 53 diagrams including NLO QCD corrections.
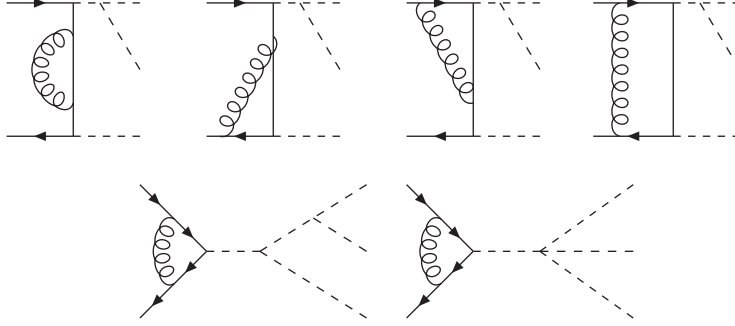
Figure 3: Additional NLO structures contributing in the production of W^+W^-Z, W^+ZZ, and $W^+W^-W^+$, that do not appear in the ZZZ case. Dashed internal lines can represent W, Z, Goldstone bosons or photons.

3. Real emission

The real emission corrections for the production process of three vector bosons

$$q + \bar{q} \to V + V + V \tag{3.1}$$

fall in the following three categories

$$q + \bar{q} \to V + V + V + g \tag{3.2}$$

$$g + q \to V + V + V + q \tag{3.3}$$

$$g + \bar{q} \to V + V + V + \bar{q} \quad . \tag{3.4}$$

IR divergences arise if a massless final state particle becomes soft or collinear to an initial parton. We deal with the IR part of the calculation by using the two cut-off phase space slicing method [39, 40] and the dipole formalism of Catani and Seymour [36]. Let us first provide the relevant formulas for the dipole subtraction method.

3.1 Dipole subtraction

The partonic cross section at the NLO level consists of Born term (B), virtual corrections (V), collinear counter terms (C) defined on the 3-particle phase space and the real emission corrections (R). Dipole terms (A) which approximate the real emission matrix elements in all soft/collinear regions are subtracted from the real matrix element before integration over the four-particle phase space. The same terms are added back, integrated over the dimensionally regulated phase space of

the soft/collinear particle:

$$\sigma_{q\bar{q}}^{NLO} = \int_{V\bar{V}Vg} \left[d\sigma_{q\bar{q}}^{R} - d\sigma_{q\bar{q}}^{A}\right] + \int_{V\bar{V}V} \left[d\sigma_{q\bar{q}}^{B} + d\sigma_{q\bar{q}}^{V} + \int_{g} d\sigma_{q\bar{q}}^{A} + d\sigma_{q\bar{q}}^{C}\right] \quad . \tag{3.5}$$

After subtracting the dipole terms the real emission cross section is finite and can be evaluated in 4 dimensions. The same is true for the other terms after the pole parts have been canceled.

The colour averaged leading order contribution is given by

$$d\sigma_{q\bar{q}}^{B} = \frac{C_S}{N} \frac{1}{2s_{12}} |\mathcal{M}^{B}|^2 \, d\Phi_{VVV} \tag{3.6}$$

where $\mathcal{M}^{B}$ is the kinematic part of the leading order amplitude and $s_{12} = 2p_1 \cdot p_2$. If two (three) vector bosons are identical a symmetry factor $C_S = 1/2$ ($C_S = 1/6$) has to be included. The three particle phase space of the vector bosons is denoted as $d\Phi_{VVV}$. The real emission corrections are defined on the four particle phase space $d\Phi_{VVVx}$ where x can be either g, q, or $\bar{q}$.

In the case of a $q\bar{q}$ initial state two dipoles are needed as subtraction terms. The subtraction term for the gluon emission off the quark (neglecting $\mathcal{O}(\epsilon)$ terms) is

$$\mathcal{D}^{q_1 g_6, \bar{q}_2} = \frac{8\pi\alpha_s C_F}{2\tilde{x} \, p_1 \cdot p_6} \left(\frac{1 + \tilde{x}^2}{1 - \tilde{x}}\right) |\mathcal{M}_{q\bar{q}}^{B}(\tilde{p}_{16}, p_2, \tilde{p}_3, \tilde{p}_4, \tilde{p}_5)|^2 \tag{3.7}$$

where

$$\tilde{x} = \frac{p_1 \cdot p_2 - p_2 \cdot p_6 - p_1 \cdot p_6}{p_1 \cdot p_2}$$

$$\tilde{p}_{16} = \tilde{x} \, p_1 \quad , \quad K = p_1 + p_2 - p_6 \quad , \quad \tilde{K} = \tilde{p}_{16} + p_2$$

$$\Lambda^{\mu\nu} = g^{\mu\nu} - \frac{2(K^\mu + \tilde{K}^\mu)(K^\nu + \tilde{K}^\nu)}{(K + \tilde{K})^2} + \frac{2\tilde{K}^\mu K^\nu}{K^2}$$

$$\tilde{p}_j = \Lambda \, p_j \tag{3.8}$$

defines the dipole kinematics: $q(\tilde{p}_{16}) + \bar{q}(p_2) \rightarrow V(\tilde{p}_3) + V(\tilde{p}_4) + V(\tilde{p}_5)$. The subtraction term for gluon emission off the anti-quark is obtained by interchanging $p_1 \leftrightarrow p_2$. The real emission cross section including subtraction terms reads

$$d\sigma_{q\bar{q}}^{R} - d\sigma_{q\bar{q}}^{A} = \frac{C_S}{N} \frac{1}{2s_{12}} \left[C_F \, |\mathcal{M}_{q\bar{q}}^{R}|^2 - \mathcal{D}^{q_1 g_6, \bar{q}_2} - \mathcal{D}^{\bar{q}_2 g_6, q_1}\right] d\Phi_{VVVg} \tag{3.9}$$

The part of the NLO cross section which is defined on the $2 \rightarrow 3$ phase space is obtained after analytic integration of the dipole terms over the phase space of the unresolved particle. A collinear counter term is added to treat the collinear $1/\epsilon$ pole which is absorbed into the parton distribution

functions at a scale μ_F. All details can be found in [36]. The part which has to be added to the virtual corrections is given by

$$d\sigma_{q\bar{q}}^C + \int_g d\sigma_{q\bar{q}}^A = \frac{\alpha_s C_F}{2\pi} \frac{\Gamma(1+\epsilon)}{(4\pi)^{-\epsilon}} \left(\frac{s_{12}}{\mu^2}\right)^{-\epsilon} \left[\frac{2}{\epsilon^2} + \frac{3}{\epsilon} - \frac{2\pi^2}{3}\right] d\sigma_{q\bar{q}}^B$$

$$+\frac{\alpha_s C_F}{2\pi} \int_0^1 dx \, \mathcal{K}^{q,q}(x) \, d\sigma_{q\bar{q}}^B(xp_1, p_2) + \frac{\alpha_s C_F}{2\pi} \int_0^1 dx \, \mathcal{K}^{\bar{q},\bar{q}}(x) \, d\sigma_{q\bar{q}}^B(p_1, xp_2) \qquad (3.10)$$

where the term

$$\mathcal{K}^{q,q}(x) = \mathcal{K}^{\bar{q},\bar{q}}(x) = \left[\frac{1+x^2}{1-x}\right]_+ \log\left(\frac{s_{12}}{\mu_F^2}\right) + \left[\frac{4\log(1-x)}{1-x}\right]_+ + (1-x) - 2(1+x)\log(1-x)$$

contains plus distributions which are defined as usual

$$\int_0^1 dx \left[\frac{g(x)}{1-x}\right]_+ f(x) = \int_0^1 dx \, g(x)\frac{f(x) - f(1)}{1-x} \qquad (3.11)$$

For initial states with a gluon no soft contribution is present and thus one has

$$\sigma_{gq}^{NLO} = \int_{V\bar{V}V} \left[\int_q d\sigma_{gq}^A + d\sigma_{gq}^C\right] + \int_{V\bar{V}Vq} \left[d\sigma_{gq}^R - d\sigma_{gq}^A\right] \qquad (3.12)$$

In this case only one subtraction term is needed, namely

$$d\sigma_{gq}^R - d\sigma_{gq}^A = \frac{C_S}{N} \frac{1}{2s_{12}} \left[T_R|\mathcal{M}_{gq}^R|^2 - \mathcal{D}^{g_1 q_6, q_2}\right] d\Phi_{V\bar{V}Vq} \quad , \qquad (3.13)$$

where the dipole is given by

$$\mathcal{D}^{g_1 q_6, q_2} = \frac{8\pi\alpha_s}{\tilde{x}} \frac{T_R}{2\, p_1 \cdot p_6} \left[1 - 2\,\tilde{x}\,(1-\tilde{x})\right] |\mathcal{M}_{q\bar{q}}^B(\tilde{p}_j)|^2 \quad . \qquad (3.14)$$

The momentum mappings $\tilde{p}_j$ are identical to the ones in Eq. (3.8).

The initial state collinear singularity is again absorbed by the pdfs through a counter term

$$d\sigma_{gq}^C + \int_q d\sigma_{gq}^A = \frac{\alpha_s T_R}{2\pi} \int_0^1 dx \, \mathcal{K}^{g,q}(x) \, d\sigma_{q\bar{q}}^B(xp_1, p_2)$$

$$\mathcal{K}^{g,q}(x) = [x^2 + (1-x)^2]\log\left(\frac{s_{12}}{\mu_F^2}\right) + 2x(1-x) + 2[x^2 + (1-x)^2]\log(1-x) \quad . \qquad (3.15)$$

The formulas for the cases qg, $\bar{q}g$, $g\bar{q}$ are identical up to relabeling of momenta.

The hadronic differential cross section with hadron momenta P_1 and P_2 is the sum over all partonic initial states convoluted with the parton distribution functions

$$d\sigma(P_1, P_2) = \sum_{ab} \int dz_1 dz_2 f_a(z_1, \mu_F) f_b(z_2, \mu_F) d\sigma_{ab}(z_1 P_1, z_2 P_2) \tag{3.16}$$

The sum runs over the six partonic configurations $q\bar{q}$, $\bar{q}q$, gq, qg, $g\bar{q}$, $\bar{q}g$.

3.2 Phase space slicing

To have an independent check for the real radiation we have also implemented the phase space slicing method in its two cut-off variant [39, 40]. One splits the phase space in soft, collinear and hard regions with the help of the cut-off parameters δ_s and δ_c. In the soft region the $2 \to 4$ matrix element is replaced by the eikonal approximation. In the collinear region one has a convolution of a splitting function with the Born term. Adding the soft/collinear parts to the virtual corrections all poles cancel and one obtains the three-particle contribution

$$\sigma^{(3)} = \left(\frac{\alpha_s}{2\pi}\right) \sum_{a,b} \int dz_1 dz_2 d\sigma_{ab}^B \left[f_a(z_1, \mu_F) f_b(z_2, \mu_F) \left(A_0^s + A_0^v + 2A_0^{sc}\right) \right.$$
$$\left. + f_a(z_1, \mu_F)\widetilde{f_b}(z_2, \mu_F) + \widetilde{f_a}(z_1, \mu_F)f_b(z_2, \mu_F)\right] \tag{3.17}$$

with

$$A_0^s = 4\ln^2 \delta_s\, C_F$$
$$A_0^{sc}(q \to qg) = C_F \left(2\ln\delta_s + 3/2\right)\ln\frac{s_{12}}{\mu_f^2}$$
$$A_0^v = \frac{d\sigma_{ab}^V}{d\sigma_{ab}^B}\,. \tag{3.18}$$

The $\widetilde{f}$ functions are given by

$$\widetilde{f_a}(x, \mu_F) = \sum_b \int_x^{1-\delta_s\delta_{ab}} \frac{dz}{z} f_b(x/z, \mu_F)\widetilde{P}_{ab}(z)\,. \tag{3.19}$$

where

$$\widetilde{P}_{ab}(z) = P_{ab}(z)\ln\left(\delta_c \frac{1-z}{z}\frac{2xp_1 \cdot p_2}{\mu_F^2}\right) - P'_{ab}(z)\,. \tag{3.20}$$

The upper limit $1 - \delta_s$ ensures that the soft region which is already dealt with is excluded. The Kronecker δ_{ab} indicates that for $a \neq b$ there is only a collinear divergence and no soft cut-off is needed.

In our case we need only the splitting functions $P_{qq}(z)$ and $P_{gq}(z)$. If we write $P_{ab}(z, \epsilon) = P_{ab}(z) + \epsilon P'_{ab}(z)$, we have

$$P_{qq}(z) = C_F \frac{1 + z^2}{1 - z} \tag{3.21}$$

$$P'_{qq}(z) = -C_F(1 - z)$$

$$P_{gq}(z) = T_R \left(z^2 + (1 - z)^2\right)$$

$$P'_{gq}(z) = -2\,T_R\,z(1 - z)$$

We see that the $\widetilde{f}$ functions contain an explicit logarithm of δ_c as well as logarithmic dependencies on δ_s which are built up by the integration on z_1, z_2.

The four-body contribution is given by

$$\sigma^{(4)} = \sum_{a,b=\bar{q},q,g} \int dz_1 dz_2 f_a(z_1, \mu_F) f_b(z_2, \mu_F) d\hat{\sigma}^R_{ab}, \tag{3.22}$$

with the hard-non-collinear partonic cross section given by

$$d\hat{\sigma}_{ab} = \frac{C_S}{2 s_{12}} \int_{H\overline{C}} \overline{\sum} |\mathcal{M}_{ab}|^2 d\Phi_{VVVx}, \tag{3.23}$$

where $\overline{\sum} |\mathcal{M}^R|^2$ is the two-to-four body squared matrix element averaged (summed) over initial (final) degrees of freedom, $d\Phi_{VVVx}$ is the four-body phase space and the hard non-collinear region denoted by $H\overline{C}$ is defined by

$$E_6 > \delta_s \frac{\sqrt{s_{12}}}{2}$$

$$2p_1 \cdot p_6, 2p_2 \cdot p_6 > \delta_c\, s_{12} \tag{3.24}$$

where p_6 is the momentum of the soft/collinear parton with energy E_6.

Both methods have been implemented in `HELAC`[45]. The results show excellent agreement between the two methods. In the numerical results presented below we only show the results of the dipole subtraction approach.

4. Numerical results

We present in this Section a selection of the results that we obtained for the four processes studied in this paper.

The complete virtual part of the next-to-leading order calculation for the four processes studied in this paper has been performed using `CutTools` [35] and also checked against an independent code.

The two programs provide identical results for the amplitudes studied. As further tests, we checked that the tree-level results obtained using Feynman diagrams coincides with the results obtained with HELAC[45] and that we reconstruct the correct structure for the poles after integration. Concerning the finite parts, we agree with the results obtained by the authors of Ref. [16], for the production of three Z bosons. In this section we will mostly focus on the processes for which no results have appeared yet in the literature, namely the production of $W^+W^-W^+$ and W^+ZZ.

We use the following values for the electroweak parameters:

$$M_W = 80.4 \text{ GeV} , \ M_Z = 91.1875 \text{ GeV} , \ G_F = 1.16639 \cdot 10^{-5} \text{ GeV}^{-2} . \tag{4.1}$$

In all cases presented here, we set $\sqrt{s} = 14$ TeV and used CTEQ6L1 [44] with $\alpha_s(M_Z) = 0.129$ at NLO. For the electroweak couplings we use the the G_μ scheme with

$$\alpha_{em} = \frac{\sqrt{2} \, G_F M_W^2 \sin^2 \theta_W}{\pi} \tag{4.2}$$

and

$$\sin^2 \theta_W = 1 - M_W^2 / M_Z^2 \tag{4.3}$$

The tree-level cross section has been evaluated using the HELAC event generator[45]. The same programme, appropriately adapted, has been used to calculate also the real corrections. The virtual corrections have been calculated on the basis of unweighted tree-order events produced by HELAC with an indicative CPU time of 180 ms per event, which is quite good taking into account that the numerical calculation of one-loop amplitudes (the numerators of the OPP method) is performed using standard momentum representation of Feynman graphs without any optimization. A conservative comparison with the efficiency of the tree order calculation, based on HELAC, shows that a further improvement of the order of $10^1 - 10^2$ is to be expected.

Since the purpose of our paper is to show the feasibility of the OPP method in a realistic situation, the results we present here are indicative and they constitute by no means a detailed discussion of the phenomenology of these processes. Partial results have been already presented in [1, 34].

It should be mentioned however that all results are available as (un)weighted events, which means that an exhaustive study in the full phase space, both for three- and four-particle final states[2], poses no problem and will be postponed for the future, taking into account also decay products and intermediate Higgs contributions.

In Figure 4, we show results for the p_T distributions of all processes. For each phase space point, the p_T of each of the three bosons gives an entry in the histograms. The final result is then divided

---

[2]Of course both positive and negative contributions have been taken into account, separately.

Process	scale μ	Born cross section [fb]	NLO cross section [fb]
ZZZ	$3M_Z$	9.7(1)	15.3(1)
WZZ	$2M_Z + M_W$	20.2(1)	40.4(2)
WWZ	$M_Z + 2M_W$	96.8(6)	181.7(8)
WWW	$3M_W$	82.5(5)	146.2(6)

Table 1: Cross section for the four processes, corresponding to the distributions in Fig 4. Different values of the factorization(renormalization) scale are used for the different processes.

by 3, yielding, as a normalization factor, the total cross section. The corresponding K-factors are depicted in Figure 5. In the W^+ZZ and $W^+W^-W^+$ cases, we observe an interesting increase in the K-factor for high values of the transverse momentum.

The corresponding total cross sections are contained in Table 1. As we can see the NLO corrections are quite significant, resulting to overall K-factors of order ~ 2.

In Figure 6, we show, as an indicative case, the rapidity distribution for WWW production, which is the process with the highest cross section. Also here, each of the three bosons gives an entry in the histograms, that are eventually normalized to the total cross section.

The K-factor appears to have now an important dependence on the phase space, especially near the borders of the available rapidity region

Let us discuss now the results obtained for the production of $W^+W^-W^+$ and W^+ZZ. In Tables 2 and 3 we present the results for the cross sections (in fb) of $pp \rightarrow W^+W^-W^+$ and $pp \rightarrow W^+ZZ$, respectively. Each table contains the Born level, the NLO result and the corresponding K-factor.

scale	σ_B	σ_{NLO}	K
$\mu = M/2$	82.7(5)	153.2(6)	1.85
$\mu = M$	81.4(5)	144.5(6)	1.77
$\mu = 2M$	81.8(5)	139.1(6)	1.70

Table 2: Cross section $pp \rightarrow W^+W^-W^+$ in fb for different values of the factorization(renormalization) scale. In the table above we set $M = 3M_Z$.

5. Summary and Conclusions

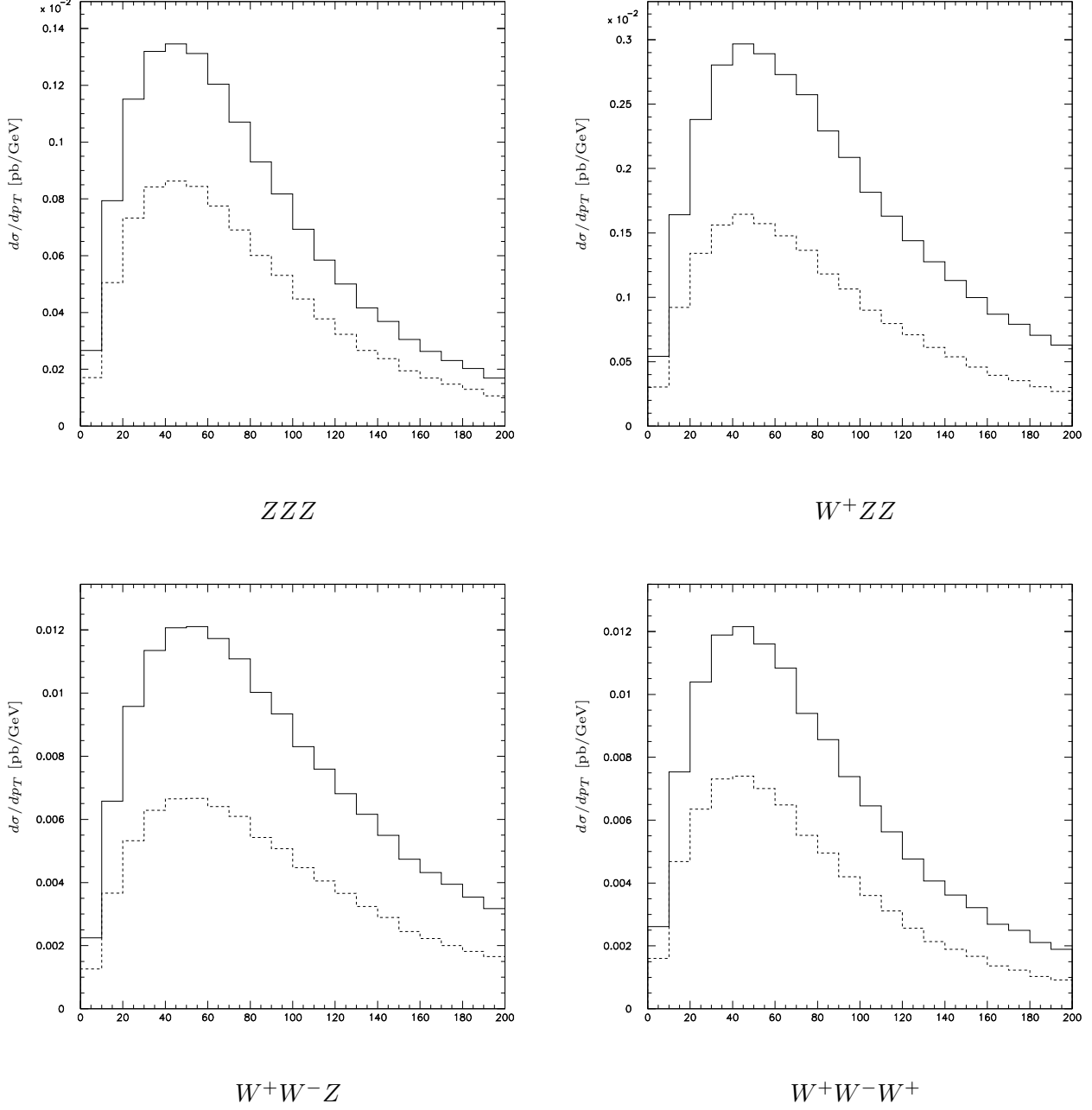In this paper we considered the production of three vector bosons at the LHC. We discussed four

Figure 4: Transverse momentum distribution, as defined in the text, for the four processes $pp \to VVV$: NLO (solid line) compared with the LO contribution (dashed line).

processes, namely ZZZ, W^+W^-Z, W^+ZZ, and $W^+W^-W^+$ production: for each process we calculated the next-to-leading order QCD corrections, presenting our results in the form of transverse
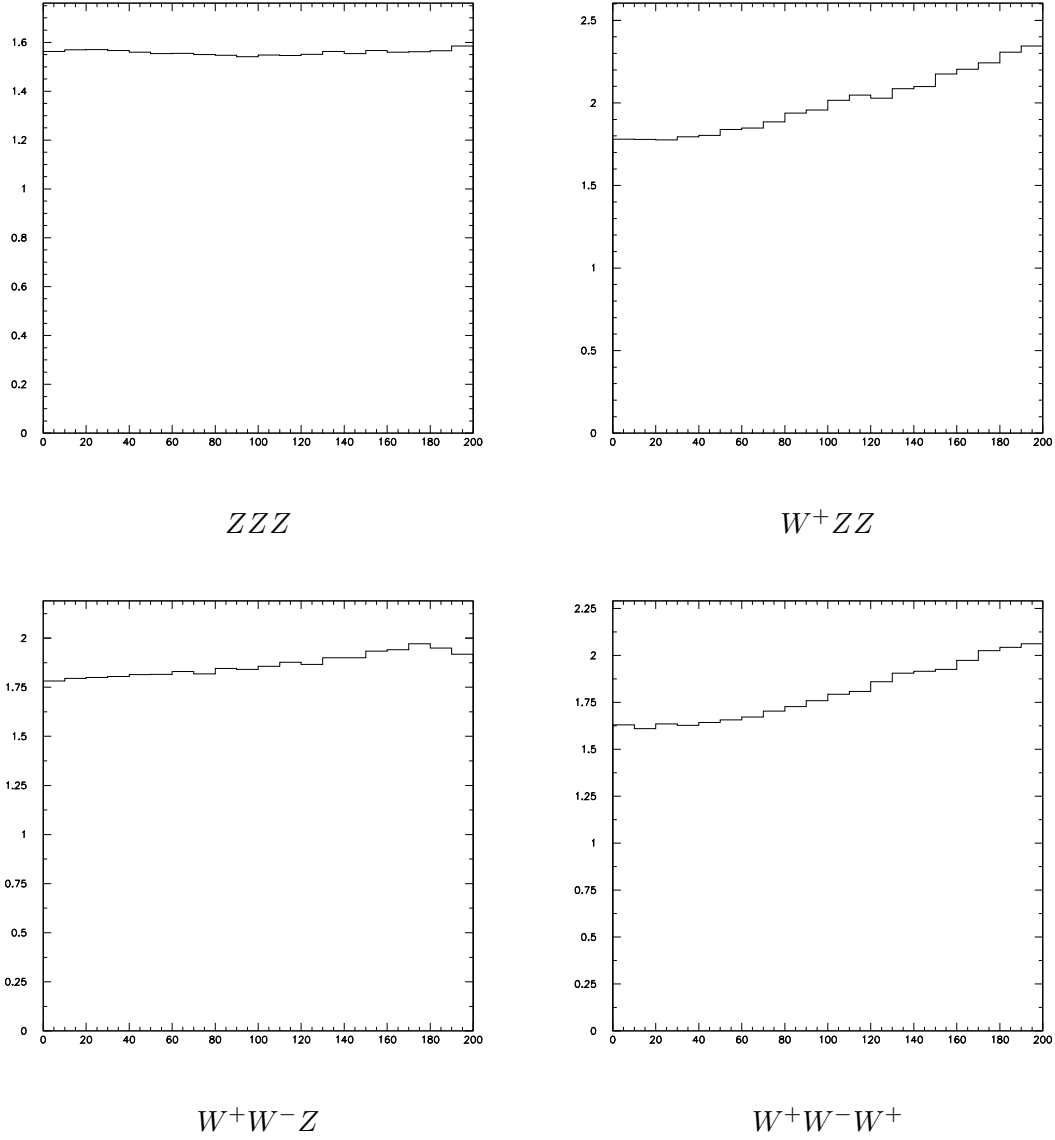
Figure 5: $K-$factors, corresponding to the plots in Fig. 4

momentum and rapidity distributions. The QCD corrections are quite sizable, with a K-factor of order 2. The K-factor is rather uniform in p_T distributions, while shows an important dependence on the phase space as far as rapidity distributions are concerned. Given the size of the corrections the QCD corrections have to be taken into account in experimental studies at the LHC.

This paper also represents the first complete calculation of physical cross-sections performed using the recently introduced OPP method for the reduction of one-loop amplitudes, in which the
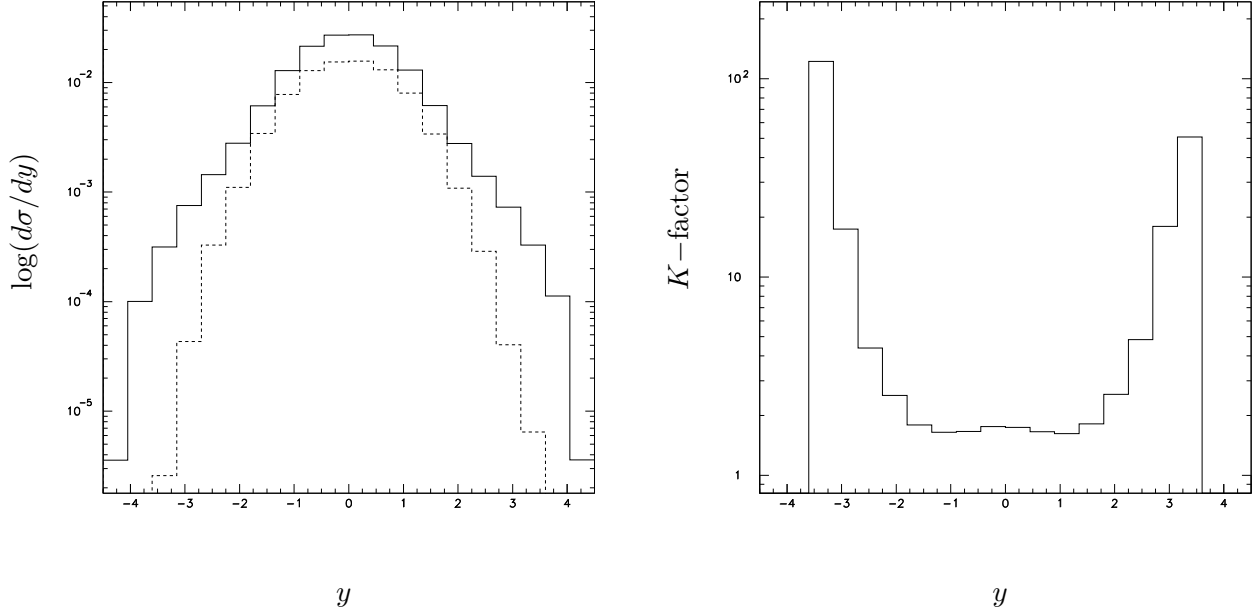
Figure 6: Rapidity distribution, as defined in the text, for $pp \to W^+W^-W^+$: on the left plot, NLO (solid line) compared with the LO contribution (dashed line) in logarithmic scale; on the right, the corresponding $K-$factor. The scale is set to $\mu = 3M_W$.

scale	σ_B	σ_{NLO}	K
$\mu = M/2$	20.2(1)	43.0(2)	2.12
$\mu = M$	20.0(1)	39.7(2)	1.99
$\mu = 2M$	19.7(1)	37.8(2)	1.91

Table 3: Cross section $pp \to W^+ZZ$ in fb for different values of the factorization(renormalization) scale. In the table above we set $M = 3M_Z$.

reduction to known integrals is performed at the integrand level, using the Fortran code `CutTools`.

The efficiency of the OPP method is quite good. It can be further improved by developing the numerical evaluation of the integrand in the one-loop amplitude by means of recursion relations [46], without relying on Feynman diagrams.

We conclude that the OPP method is a viable alternative to perform phenomenologically relevant one-loop calculations, as it does not rely on the recursive evaluation of scalar and tensor momentum integrals. Its versatility and simplicity make it a very good candidate for the construction of a universal NLO calculator/event-generator.

References

[1] Z. Bern *et al.*, *"The NLO multileg working group: summary report," Proceedings of the Les Houches 2007 workshop on Physics at TeV colliders*, arXiv:0803.0494 [hep-ph].

[2] W. T. Giele and E. W. N. Glover, JHEP **0404** (2004) 029 [arXiv:hep-ph/0402152].

[3] T. Binoth, J. P. Guillet, G. Heinrich, E. Pilon and C. Schubert, JHEP **0510** (2005) 015 [arXiv:hep-ph/0504267].

[4] A. Denner and S. Dittmaier, Nucl. Phys. B **734** (2006) 62 [arXiv:hep-ph/0509141].

[5] A. van Hameren, J. Vollinga and S. Weinzierl, Eur. Phys. J. C **41** (2005) 361 [arXiv:hep-ph/0502165].

[6] R. K. Ellis, W. T. Giele and G. Zanderighi, Phys. Rev. D **73** (2006) 014027 [arXiv:hep-ph/0508308].

[7] Z. Bern, L. J. Dixon and D. A. Kosower, Annals Phys. **322** (2007) 1587 [arXiv:0704.2798 [hep-ph]].

[8] R. Britto, B. Feng and P. Mastrolia, Phys. Rev. D **73** (2006) 105004 [arXiv:hep-ph/0602178].

[9] T. Binoth, G. Heinrich, T. Gehrmann and P. Mastrolia, Phys. Lett. B **649** (2007) 422 [arXiv:hep-ph/0703311].

[10] C. Bernicot and J. P. Guillet, arXiv:0711.4713 [hep-ph].

[11] R. K. Ellis, W. T. Giele and Z. Kunszt, arXiv:0708.2398 [hep-ph].

[12] R. Britto, B. Feng and P. Mastrolia, arXiv:0803.1989 [hep-ph].

[13] W. T. Giele, Z. Kunszt and K. Melnikov, arXiv:0801.2237 [hep-ph].

[14] M. Moretti, F. Piccinini and A. D. Polosa, arXiv:0802.4171 [hep-ph].

[15] C. F. Berger *et al.*, arXiv:0803.4180 [hep-ph].

[16] A. Lazopoulos, K. Melnikov and F. Petriello, Phys. Rev. D **76** (2007) 014001 [arXiv:hep-ph/0703273].

[17] V. Hankele and D. Zeppenfeld, arXiv:0712.3544 [hep-ph].

[18] T. Plehn and M. Rauch, Phys. Rev. D **72** (2005) 053008 [arXiv:hep-ph/0507321].

[19] T. Binoth, S. Karg, N. Kauer and R. Ruckl, Phys. Rev. D **74** (2006) 113008 [arXiv:hep-ph/0608057].

[20] B. Jager, C. Oleari and D. Zeppenfeld, JHEP **0607** (2006) 015 [arXiv:hep-ph/0603177].

[21] G. Bozzi, B. Jager, C. Oleari and D. Zeppenfeld, Phys. Rev. D **75** (2007) 073004 [arXiv:hep-ph/0701105].

[22] J. R. Andersen, T. Binoth, G. Heinrich and J. M. Smillie, arXiv:0709.3513 [hep-ph].

[23] M. Ciccolini, A. Denner and S. Dittmaier, arXiv:0710.4749 [hep-ph].

[24] A. Bredenstein, K. Hagiwara and B. Jager, arXiv:0801.4231 [hep-ph].

[25] J. M. Campbell, R. K. Ellis and G. Zanderighi, JHEP **0610** (2006) 028 [arXiv:hep-ph/0608194].

[26] M. M. Weber, Nucl. Phys. Proc. Suppl. **160** (2006) 200.

[27] S. Dittmaier, P. Uwer and S. Weinzierl, Phys. Rev. Lett. **98** (2007) 262002 [arXiv:hep-ph/0703120].

[28] G. Ossola, C. G. Papadopoulos and R. Pittau, Nucl. Phys. B **763** (2007) 147 [arXiv:hep-ph/0609007] and

[29] G. Ossola, C. G. Papadopoulos and R. Pittau, JHEP **0707** (2007) 085 [arXiv:0704.1271 [hep-ph]].

[30] F. del Aguila and R. Pittau, JHEP **0407** (2004) 017 [arXiv:hep-ph/0404120].

[31] Z. Bern, L. J. Dixon, D. C. Dunbar and D. A. Kosower, Nucl. Phys. B **435** (1995) 59 [arXiv:hep-ph/9409265].

[32] R. Britto, F. Cachazo and B. Feng, Nucl. Phys. B **725** (2005) 275 [arXiv:hep-th/0412103].

[33] W. B. Kilgore, arXiv:0711.5015 [hep-ph].

[34] G. Ossola, C. G. Papadopoulos and R. Pittau, PoS(RAD COR 2007)006.

[35] G. Ossola, C. G. Papadopoulos and R. Pittau, JHEP03(2008)042 [arXiv:0711.3596 [hep-ph]].

[36] S. Catani and M. H. Seymour, Nucl. Phys. B **485** (1997) 291 [Erratum-ibid. B **510** (1998) 503] [arXiv:hep-ph/9605323].

[37] W. T. Giele and E. W. N. Glover, Phys. Rev. D **46** (1992) 1980.

[38] W. T. Giele, E. W. N. Glover and D. A. Kosower, Nucl. Phys. B **403** (1993) 633 [arXiv:hep-ph/9302225].

[39] U. Baur, S. Keller and D. Wackeroth, Phys. Rev. D **59** (1999) 013002 [arXiv:hep-ph/9807417].

[40] B. W. Harris and J. F. Owens, Phys. Rev. D **65** (2002) 094032 [arXiv:hep-ph/0102128].

[41] P. Mastrolia, G. Ossola, C. G. Papadopoulos and R. Pittau, arXiv:0803.3964 [hep-ph].

[42] G. Ossola, C. G. Papadopoulos and R. Pittau, arXiv:0802.1876 [hep-ph].

[43] R. Pittau, Comput. Phys. Commun. **104**, 23 (1997) [arXiv:hep-ph/9607309] and **111** (1998) 48 [arXiv:hep-ph/9712418].

[44] J. Pumplin, D. R. Stump, J. Huston, H. L. Lai, P. Nadolsky and W. K. Tung, JHEP **0207** (2002) 012 [arXiv:hep-ph/0201195].

[45] A. Kanaki and C. G. Papadopoulos, Comput. Phys. Commun. **132** (2000) 306 [arXiv:hep-ph/0002082].
A. Kanaki and C. G. Papadopoulos, arXiv:hep-ph/0012004.
A. Cafarella, C. G. Papadopoulos and M. Worek, arXiv:0710.2427 [hep-ph].

[46] P. Draggiotis, A. van Hameren, R. Kleiss, A. Lazopoulos, C. G. Papadopoulos and M. Worek, Nucl. Phys. Proc. Suppl. **160** (2006) 255 [arXiv:hep-ph/0607034].